

Infinite-dimensional Bayesian filtering for detection of quasi-periodic phenomena in spatio-temporal data

Arno Solin* and Simo Särkkä†

Department of Biomedical Engineering and Computational Science (BECS),
Aalto University, P.O. Box 12200, FI-00076 AALTO, Finland.

(Dated: September 4, 2013)

This paper introduces a spatio-temporal resonator model and an inference method for detection and estimation of nearly periodic temporal phenomena in spatio-temporal data. The model is derived as a spatial extension of a stochastic harmonic resonator model, which can be formulated in terms of a stochastic differential equation (SDE). The spatial structure is included by introducing linear operators, which affect both the oscillations and damping, and by choosing the appropriate spatial covariance structure of the driving time-white noise process. With the choice of the linear operators as partial differential operators, the resonator model becomes a stochastic partial differential equation (SPDE), which is compatible with infinite-dimensional Kalman filtering. The resulting infinite-dimensional Kalman filtering problem allows for a computationally efficient solution as the computational cost scales linearly with measurements in the temporal dimension. This framework is applied to weather prediction and to physiological noise elimination in fMRI brain data.

PACS numbers: 82.40.Bj, 89.75.Kd

I. INTRODUCTION

Oscillations stem from repetitive variation, typically in time, of some measure around a point or an equilibrium. This type of phenomenon is commonly encountered in natural systems, as well as in physical, biological, and chemical models [1–3]. This paper proposes a computationally effective evolution-type stochastic partial differential equation model and an inference method, which together provide a novel and efficient means of detecting and modeling latent oscillatory structures in space–time, such as physiological noise in fMRI brain data [4, 5] or temperature variation in climate models.

The proposed model can be thought of as an extension of the following simple stochastic harmonic resonator model (see, *e.g.*, [4, 6]):

$$\frac{d^2 f(t)}{dt^2} + \gamma \frac{df(t)}{dt} + \omega^2 f(t) = \xi(t), \quad (1)$$

where $\xi(t)$ is temporally white noise, γ is the damping coefficient, and the resonator frequency is defined by the angular velocity ω (rad/s). Letting the oscillation frequency change over time and including harmonics allows the modeling of more complicated periodic and quasi-periodic (almost periodic) properties (*cf.* [4, 7]).

However, the oscillatory phenomena can also contain spatial properties. This leads to a space–time model, where the process can be described by a spatial field that is evolving in time. The main contribution herein is to set up a model in which the temporal behavior has

oscillatory characteristics, such that the process can be described by a spatio-temporal resonator model:

$$\frac{\partial^2 f(\mathbf{x}, t)}{\partial t^2} + \mathcal{A} \frac{\partial f(\mathbf{x}, t)}{\partial t} + \mathcal{B} f(\mathbf{x}, t) = \xi(\mathbf{x}, t), \quad (2)$$

where \mathcal{A} and \mathcal{B} are linear operators modeling the space–time interactions in the oscillator state. Additionally, it is shown how infinite-dimensional Kalman filters and smoothers provide computationally effective means of computing the Bayesian solution for detecting and estimating the oscillations in noisy measurement data. This can be seen as a generalization of diffusive coupling models [8] to stochastic oscillating fields.

Previously, for discrete space and time, the spatio-temporal interactions in such data have been modeled, for example, with seasonal VARMA (vector autoregressive moving average) (see, *e.g.*, [9, 10]) models. However, incorporating the spatial structure and predicting new measurements in space and time is difficult, if not impossible, in these models. For continuous-valued treatment, one can resort to neural networks (see, *e.g.*, [11]), which make it possible to account for the latent structure, but provide few tools for assessing the model structure or interpreting the results.

It would also be possible to formulate the spatio-temporal model and the related Bayesian estimation problem directly in terms of Gaussian processes (GPs), for example by using periodic covariance functions [12]. Unfortunately, the direct use of this approach leads to an intractable cubic computational complexity $\mathcal{O}(T^3)$ in the number of time steps T . To some extent, it is possible to reduce this problem by using sparse approximations (see, *e.g.*, [12, 13]), but this does not solve the problem fully.

The use of *stochastic partial differential equation* (SPDE) based models to form computationally efficient solutions to Gaussian process regression problems (or equivalent Kriging problems) has recently been discussed

* arno.solin@aalto.fi; Also at Advanced Magnetic Imaging Centre (AMI), Aalto University, Finland.

† simo.sarkka@aalto.fi; Also at Advanced Magnetic Imaging Centre (AMI), Aalto University, Finland.

in [14, 15]. In particular, in [15] the authors propose a method for converting a covariance function based spatio-temporal Gaussian process regression model into an equivalent SPDE type model. The advantage of this approach is that the Bayesian inference problem of the resulting model can be solved using infinite-dimensional Kalman filtering and smoothing with linear computational complexity in time.

This work follows an approach similar to [15], except that the SPDE model is formulated directly as a linear combination of spatio-temporal oscillators, rather than first forming a covariance function-based Gaussian process regression problem and then converting it into an SPDE. Although some modeling freedom is lost in the present approach, the advantage is that it always produces a model that can be solved with a linear time complexity algorithm, and no additional conversion procedures are required to achieve this.

The following sections introduce the spatio-temporal resonator model and explain how to select the spatial operators. The operators are chosen such that an orthogonal basis for the model can be formed by using the eigenvalue decomposition of the Laplace operator. The Hilbert space method approach to solving the GP model using Kalman filtering is discussed in brief together with maximum likelihood parameter estimation. As a proof-of-concept demonstration a one-dimensional example is presented. The method is also applied to empirical weather data (on a spherical surface) and brain data (in a polar 2D domain).

II. METHODS

A. Spatio-Temporal Resonator Model

A model for a general oscillatory phenomenon is constructed as a superposition of several resonators (separate resonators and their harmonics) with known angular velocities ω_j (*i.e.* frequencies), but unknown phases and amplitudes. These are modeled as spatially independent realizations of stochastic processes. The sum $\sum_{j=1}^N f_j(\mathbf{x}, t)$ of the oscillatory components $f_j(\mathbf{x}, t)$ can be defined using separate state space models. The spatially independent version of such a resonating field can be presented as a partial differential equation (see Eq. (1), or [4] for details):

$$\frac{\partial^2 f_j(\mathbf{x}, t)}{\partial t^2} + \gamma_j \frac{\partial f_j(\mathbf{x}, t)}{\partial t} + \omega_j^2 f_j(\mathbf{x}, t) = \xi_j(\mathbf{x}, t),$$

where $\mathbf{x} \in \Omega$ (for some domain $\Omega \subseteq \mathbb{R}^n$) denotes the spatial variable and $t \in \mathbb{R}_+$ represents time. The perturbation term $\xi_j(\mathbf{x}, t)$ is white noise, both spatially and temporally. The above formulation also contains a damping factor γ_j , which was assumed to be zero in [4].

Here, this formulation is extended to account for spatial structure by assuming that the local derivative depends not only on time, but also on surrounding locations

through some spatial linear operator. Including linear operators that affect both the oscillation and damping results in:

$$\frac{\partial^2 f_j(\mathbf{x}, t)}{\partial t^2} + \mathcal{A}_j \frac{\partial f_j(\mathbf{x}, t)}{\partial t} + \mathcal{B}_j f_j(\mathbf{x}, t) = \xi_j(\mathbf{x}, t). \quad (3)$$

This model contains three types of spatial dependency. The selection of operators \mathcal{A}_j and \mathcal{B}_j allows the suitable definition of spatial coupling through the first and second temporal derivative. Some spatial and temporal structure can also be assumed in the process noise term $\xi_j(\mathbf{x}, t)$ through a correlation structure:

$$C_j(\mathbf{x}, \mathbf{x}') = \mathbb{E}[\xi_j(\mathbf{x}, t)\xi_j(\mathbf{x}', t')] = C_{\xi_j}(\mathbf{x}, \mathbf{x}') \delta(t - t').$$

B. Choosing Spatial Operators

If the operators \mathcal{A}_j and \mathcal{B}_j are assumed to be translation and time invariant, the corresponding Fourier domain transfer functions $A_j(i\boldsymbol{\nu}_x)$ and $B_j(i\boldsymbol{\nu}_x)$ can be calculated. Taking both spatial and temporal Fourier transforms of Eq. (3) results in:

$$(i\nu_t)^2 F_j(i\boldsymbol{\nu}_x, i\nu_t) + (i\nu_t) A_j(i\boldsymbol{\nu}_x) F_j(i\boldsymbol{\nu}_x, i\nu_t) + B_j(i\boldsymbol{\nu}_x) F_j(i\boldsymbol{\nu}_x, i\nu_t) = \Xi_j(i\boldsymbol{\nu}_x, i\nu_t).$$

Solving F_j from above provides:

$$F_j(i\boldsymbol{\nu}_x, i\nu_t) = \frac{\Xi_j(i\boldsymbol{\nu}_x, i\nu_t)}{(i\nu_t)^2 + (i\nu_t) A_j(i\boldsymbol{\nu}_x) + B_j(i\boldsymbol{\nu}_x)},$$

which corresponds to the spectral density:

$$S_j(i\boldsymbol{\nu}_x, i\nu_t) = \frac{Q_j(\boldsymbol{\nu}_x)}{\|(i\nu_t)^2 + (i\nu_t) A_j(i\boldsymbol{\nu}_x) + B_j(i\boldsymbol{\nu}_x)\|^2},$$

where $Q_j(\boldsymbol{\nu}_x) = |\Xi_j(i\boldsymbol{\nu}_x, i\nu_t)|^2$ is the spectral density of ξ_j . If the operators \mathcal{A}_j and \mathcal{B}_j are assumed to be formally Hermitian, the identities $A_j(i\boldsymbol{\nu}_x) = A_j(-i\boldsymbol{\nu}_x)$ and $B_j(i\boldsymbol{\nu}_x) = B_j(-i\boldsymbol{\nu}_x)$ hold, which simplifies the spectral density to:

$$S_j(i\boldsymbol{\nu}_x, i\nu_t) = \frac{Q_j(\boldsymbol{\nu}_x)}{[\nu_t^2 - B_j(i\boldsymbol{\nu}_x)]^2 + \nu_t^2 A_j^2(i\boldsymbol{\nu}_x)}.$$

The divisor derivative zeros of the system suggest that the system has a temporal resonance of $\nu_t^2 = B_j(i\boldsymbol{\nu}_x) - A_j^2(i\boldsymbol{\nu}_x)/2$. The temporal oscillation is included in the angular velocity of ω_j by setting $B_j(i\boldsymbol{\nu}_x) = A_j^2(i\boldsymbol{\nu}_x)/2 + \omega_j^2$. This gives the spectral density in the form:

$$S_j(\boldsymbol{\nu}_x, \nu_t) = \frac{Q_j(\boldsymbol{\nu}_x)}{(\nu_t^2 - A_j^2(i\boldsymbol{\nu}_x)/2 - \omega_j^2)^2 + \nu_t^2 A_j^2(i\boldsymbol{\nu}_x)}.$$

According to Bochner's theorem [16] every positive definite function is the Fourier transform of a Borel measure.

This requires the spectral density to be positive everywhere in order to be a valid Fourier transform of a covariance function. This condition is fulfilled if $Q_j(\boldsymbol{\nu}_x)$ is a positive function (*i.e.* a valid spectral density). To ensure the causality and stability of the system $A_j(i\boldsymbol{\nu}_x)$ must be chosen such that it is a positive function, which corresponds to the operator \mathcal{A}_j being positive (semi)definite. The operator \mathcal{B}_j is also chosen to be positive, which results in the condition $A_j^2(i\boldsymbol{\nu}_x)/2 + \omega_j^2 \geq 0$. This holds, if A_j is real and positive. Zero values in the spectrum correspond to infinite peaks. However, this does not seem to be a problem, because if both operators are zero the model falls back to being spatially independent, where the only spatial structure comes from the process noise term $\xi(\mathbf{x}, t)$.

To make the model actually useful, some choices must be made. The coupling of \mathcal{A}_j and \mathcal{B}_j is determined by the condition $\mathcal{B}_j = \mathcal{A}_j^2/2 + \omega_j^2$, and the operator \mathcal{A}_j must be positive semidefinite. Examples of such operators are the identity operator \mathcal{I} and the negative Laplacian $-\Delta = -\nabla^2$. Therefore, the following operator structure is considered:

$$\begin{aligned} \mathcal{A}_j &= \gamma_j \mathcal{I} - \chi_j \nabla^2 \\ \mathcal{B}_j &= \frac{1}{2}(\gamma_j - \chi_j \nabla^2)^2 + \omega_j^2 \\ &= \frac{\gamma_j^2}{2} - \gamma_j \chi_j \nabla^2 + \frac{\chi_j^2}{2} \nabla^4 + \omega_j^2, \end{aligned} \quad (4)$$

where $\gamma_j, \chi_j \geq 0$ are some non-negative constants and ∇^4 is the so-called biharmonic operator.

A covariance function for $\xi_j(\mathbf{x}, t)$ must be chosen, which can be virtually any spatial stationary covariance function

$$E[\xi_j(\mathbf{x}, t)\xi_j(\mathbf{x}', t')] = C_{\xi,j}(\mathbf{x} - \mathbf{x}') \delta(t - t').$$

In theory, the covariance function $C_{\xi,j}$ could also be non-stationary.

C. Modeling Spatio-Temporal Data

Combining all the components in the model provides the solution as a superposition of all the oscillator components $f(\mathbf{x}, t) = \sum_{j=1}^N f_j(\mathbf{x}, t)$. The oscillator component $f_j(\mathbf{x}, t)$ is defined by a stochastic partial differential equation with the Dirichlet boundary conditions:

$$\frac{\partial^2 f_j(\mathbf{x}, t)}{\partial t^2} + \mathcal{A}_j \frac{\partial f_j(\mathbf{x}, t)}{\partial t} + \mathcal{B}_j f_j(\mathbf{x}, t) = \xi_j(\mathbf{x}, t),$$

for $(\mathbf{x}, t) \in \Omega \times \mathbb{R}_+$, and $f_j(\mathbf{x}, t) = 0$ for $(\mathbf{x}, t) \in \partial\Omega \times \mathbb{R}_+$, for all $j = 1, 2, \dots, N$. The state of the system is defined as a combination of the periodic oscillating fields and their first temporal derivatives:

$$\mathbf{f}(\mathbf{x}, t) = [f_1(\mathbf{x}, t) \frac{\partial}{\partial t} f_1(\mathbf{x}, t) \dots f_N(\mathbf{x}, t) \frac{\partial}{\partial t} f_N(\mathbf{x}, t)]^\top.$$

This leads to the linear state space model, which can be expressed in the following form:

$$\begin{aligned} \frac{\partial \mathbf{f}(\mathbf{x}, t)}{\partial t} &= \mathcal{F} \mathbf{f}(\mathbf{x}, t) + \mathbf{L} \xi(\mathbf{x}, t) \\ \mathbf{y}_k &= \mathcal{H}_k \mathbf{f}(\mathbf{x}, t_k) + \mathbf{r}_k, \end{aligned} \quad (5)$$

where \mathcal{F} is a block-diagonal matrix such that each block j consists of a 2×2 matrix of linear operators, and \mathbf{L} is a block-diagonal matrix consisting of 2×1 blocks:

$$\mathcal{F}_j = \begin{bmatrix} 0 & \mathcal{I} \\ -\mathcal{B}_j & -\mathcal{A}_j \end{bmatrix} \quad \text{and} \quad \mathbf{L}_j = \begin{bmatrix} 0 \\ 1 \end{bmatrix}.$$

In step k , the observed values are $\mathbf{y}_k \in \mathbb{R}^{d_k}$. The measurement model is constructed by defining a functional \mathcal{H}_k through which the model is observed at discrete time steps t_k at known locations $\mathbf{x}_i^{\text{obs}} \in \Omega, i = 1, 2, \dots, d_k$, that is $\mathbf{f} \mapsto \mathbf{f}(\mathbf{x}^{\text{obs}}, t_k)$. The measurement noise term $\mathbf{r}_k \sim \mathcal{N}(\mathbf{0}, \mathbf{R}_k)$ in Eq. (5) is a Gaussian random variable of dimension d_k . For notational convenience, the possibility of \mathcal{F} depending on time has been omitted. However, it is included in one of the demonstrations, where the oscillation frequencies in $\omega_j(t)$ change over time.

D. Infinite-Dimensional Kalman Filtering

The Kalman filter (see, *e.g.*, [17]) is an algorithm for solving the state estimation problem, which refers to the inverse problem of estimating the state trajectory of the stochastic process $\mathbf{f}(\mathbf{x}, t)$ based on the noisy observations $\mathbf{y}_1, \mathbf{y}_2, \dots, \mathbf{y}_k$. The Kalman filter solution is the statistically optimal solution in a Bayesian sense given the model of the system.

Eq. (5) is the infinite-dimensional counterpart of a continuous-time state space model, where the linear matrix evolution equation has been replaced by a linear differential operator equation (*cf.* [15]). The first equation (the dynamic model) in (5) is an infinite-dimensional linear stochastic differential equation [16]. Here, \mathcal{F} is a differential operator, and the equation is an *evolution type* stochastic partial differential equation (SPDE) [16, 18].

Treating the temporal variable separately in the evolution type SPDE enables the use of infinite-dimensional optimal estimation methods. However, these methods are meant for discrete time estimation, and therefore the evolution equation needs to be discretized with respect to time. First, the evolution operator is formed:

$$\mathbf{U}(\Delta t) = \exp(\Delta t \mathcal{F}),$$

where $\exp(\cdot)$ is the operator exponential function. A solution to the stochastic equation can now be given as (see [15, 16] for details):

$$\begin{aligned} \mathbf{f}(\mathbf{x}, t_{k+1}) &= \mathbf{U}(t_{k+1} - t_k) \mathbf{f}(\mathbf{x}, t_k) \\ &+ \int_{t_k}^{t_{k+1}} \mathbf{U}(t_{k+1} - \tau) \mathbf{L} \xi(\mathbf{x}, \tau) \, d\tau, \end{aligned} \quad (6)$$

where t_{k+1} and $t_k < t_{k+1}$ are arbitrary. The second term is a Gaussian process with covariance function $\mathbf{Q}(\mathbf{x}, \mathbf{x}'; t_k, t_{k+1}) = \int_{t_k}^{t_{k+1}} \mathbf{U}(t_{k+1} - \tau) \mathbf{L} \mathbf{C}_\xi(\mathbf{x}, \mathbf{x}') \mathbf{L}^\top \mathbf{U}^*(t_{k+1} - \tau) d\tau$. This leads to the following discrete-time model:

$$\begin{aligned} \mathbf{f}(\mathbf{x}, t_k) &= \mathbf{U}(\Delta t_k) \mathbf{f}(\mathbf{x}, t_{k-1}) + \mathbf{q}_k(\mathbf{x}) \\ \mathbf{y}_k &= \mathcal{H}_k \mathbf{f}(\mathbf{x}, t_k) + \mathbf{r}_k, \end{aligned} \quad (7)$$

where $\Delta t_k = t_k - t_{k-1}$ and the process noise $\mathbf{q}_k(\mathbf{x}) \sim \mathcal{GP}(\mathbf{0}, \mathbf{Q}(\mathbf{x}, \mathbf{x}'; \Delta t_k))$. This discretization is not an approximation, but is the so-called *mild solution* to the infinite-dimensional differential equation [16].

1. Infinite-Dimensional Kalman Filter and Smoother

The *infinite-dimensional Kalman filter* [19–21] is a closed-form solution to the infinite-dimensional linear filtering problem (7). Here, a two-step scheme is presented, which first calculates the marginal distribution of the next step using the known system dynamics. The following formulation uses a notation similar to [15] and can be compared to the finite-dimensional Kalman filter [22].

The infinite-dimensional **prediction step** can be expressed as follows:

$$\begin{aligned} \mathbf{m}_{k|k-1}(\mathbf{x}) &= \mathbf{U}(\Delta t_k) \mathbf{m}_{k-1|k-1}(\mathbf{x}) \\ \mathbf{C}_{k|k-1}(\mathbf{x}, \mathbf{x}') &= \mathbf{U}(\Delta t_k) \mathbf{C}_{k-1|k-1}(\mathbf{x}, \mathbf{x}') \mathbf{U}^*(\Delta t_k) \\ &\quad + \mathbf{Q}(\mathbf{x}, \mathbf{x}'; \Delta t_k), \end{aligned} \quad (8)$$

where $(\cdot)^*$ denotes an adjoint, which in practice swaps the roles of inputs \mathbf{x} and \mathbf{x}' , and operates from the right. The operator adjoint can be seen as an operator version of a matrix transpose. The recursive iteration is initialized by presenting the prior information in the form $\mathbf{f}(\mathbf{x}, t_0) \sim \mathcal{GP}(\mathbf{m}_0(\mathbf{x}), \mathbf{C}_0(\mathbf{x}, \mathbf{x}'))$.

The algorithm then uses each observation to update the distribution to match the new information obtained by the measurement in step k . This is the infinite-dimensional **update step**:

$$\begin{aligned} \mathbf{S}_k &= \mathcal{H}_k \mathbf{C}_{k|k-1}(\mathbf{x}, \mathbf{x}') \mathcal{H}_k^* + \mathbf{R}_k \\ \mathbf{K}_k(\mathbf{x}) &= \mathbf{C}_{k|k-1}(\mathbf{x}, \mathbf{x}') \mathcal{H}_k^* \mathbf{S}_k^{-1} \\ \mathbf{m}_{k|k}(\mathbf{x}) &= \mathbf{m}_{k|k-1}(\mathbf{x}) + \mathbf{K}_k(\mathbf{x}) (\mathbf{y}_k - \mathcal{H}_k \mathbf{m}_{k|k-1}(\mathbf{x})) \\ \mathbf{C}_{k|k}(\mathbf{x}, \mathbf{x}') &= \mathbf{C}_{k|k-1}(\mathbf{x}, \mathbf{x}') - \mathbf{K}_k(\mathbf{x}) \mathbf{S}_k \mathbf{K}_k^*(\mathbf{x}), \end{aligned} \quad (9)$$

where $(\cdot)^{-1}$ denotes the matrix inverse. As a result, the filtered forward-time posterior process in step k (time t_k) is given by $\mathbf{f}_{k|k}(\mathbf{x}) \sim \mathcal{GP}(\mathbf{m}_{k|k}(\mathbf{x}), \mathbf{C}_{k|k}(\mathbf{x}, \mathbf{x}'))$.

The purpose of optimal (fixed-interval) smoothing is to obtain in closed-form the marginal posterior distribution of the state \mathbf{f}_k in time step t_k , which is conditional on all the measurements $\mathbf{y}_{1:T}$, where $k \in [1, \dots, T]$ is a fixed interval.

The infinite-dimensional Rauch–Tung–Striebel (RTS) smoother equations are written so that they utilize the Kalman filtering results $\mathbf{m}_{k|k}(\mathbf{x})$ and $\mathbf{C}_{k|k}(\mathbf{x}, \mathbf{x}')$ as a forward sweep, and then perform a backward sweep to update the estimates to match the forthcoming observations. The smoother’s backward sweep may be expressed with the following infinite-dimensional **RTS smoothing equations** [15]:

$$\begin{aligned} \mathbf{m}_{k+1|k}(\mathbf{x}) &= \mathbf{U}(\Delta t_k) \mathbf{m}_{k|k}(\mathbf{x}) \\ \mathbf{C}_{k+1|k}(\mathbf{x}, \mathbf{x}') &= \mathbf{U}(\Delta t_k) \mathbf{C}_{k|k}(\mathbf{x}, \mathbf{x}') \mathbf{U}^*(\Delta t_k) \\ &\quad + \mathbf{Q}_k(\mathbf{x}, \mathbf{x}'; \Delta t_k) \\ \mathcal{G}_k &= \mathbf{C}_{k|k}(\mathbf{x}, \mathbf{x}') \mathbf{U}^*(\Delta t_k) [\mathbf{C}_{k+1|k}(\mathbf{x}, \mathbf{x}')]^{-1} \\ \mathbf{m}_{k|T}(\mathbf{x}) &= \mathbf{m}_{k|k}(\mathbf{x}) \\ &\quad + \mathcal{G}_k [\mathbf{m}_{k+1|T}(\mathbf{x}) - \mathbf{m}_{k+1|k}(\mathbf{x})] \\ \mathbf{C}_{k|T}(\mathbf{x}, \mathbf{x}') &= \mathbf{C}_{k|k}(\mathbf{x}, \mathbf{x}') + \mathcal{G}_k (\mathbf{C}_{k+1|T}(\mathbf{x}, \mathbf{x}') \\ &\quad - \mathbf{C}_{k+1|k}(\mathbf{x}, \mathbf{x}')) \mathcal{G}_k^*. \end{aligned} \quad (10)$$

In the above equations, $(\cdot)^{-1}$ denotes the operator inverse. In addition, note that \mathcal{G}_k is a linear operator whose kernel is defined via the covariance kernels of the filtering results. This makes the notation slightly more challenging.

Once both the Kalman filtering and Rauch–Tung–Striebel sweeps are performed on the model given the observed data, the marginal posterior is obtained, which can be represented as the Gaussian process:

$$\mathbf{f}(\mathbf{x}, t_k | \mathbf{y}_{1:T}) \sim \mathcal{GP}(\mathbf{m}_{k|T}(\mathbf{x}), \mathbf{C}_{k|T}(\mathbf{x}, \mathbf{x}')),$$

where the observed values $\mathbf{y}_k \in \mathbb{R}^{d_k}$ are given at discrete time points $t_k, k = 1, 2, \dots, T$, and measured at known locations $\mathbf{x}_{i,k}^{\text{obs}} \in \Omega, i = 1, \dots, d_k$. The resulting process functions can be evaluated at any test point $\mathbf{x}_* \in \Omega$ by simply considering an appropriate measurement functional \mathcal{H} . Thus, the marginal posterior of the value of $\mathbf{f}(\mathbf{x}_*, t_k)$ in \mathbf{x}_* at time instant t_k is:

$$\begin{aligned} p(\mathbf{f}(\mathbf{x}_*, t_k) | \mathbf{y}_{1:T}) &= \\ &\quad \mathcal{N}(\mathbf{f}(\mathbf{x}_*, t_k) | \mathbf{m}_{k|T}(\mathbf{x}_*), \mathbf{C}_{k|T}(\mathbf{x}_*, \mathbf{x}_*)). \end{aligned}$$

Values could also be predicted at more time steps. A test time point t_* should be taken into account when performing the time discretization. The state of the system $\mathbf{f}(\mathbf{x}, t_*)$ would be predicted in this step, but because there are no data, no updating step is needed.

One detail worthy of note is the connection between the standard (in this case) spatial GP model and the evolution type state space SPDE. If the temporal evolution model is left out, that is $\mathcal{F} = 0$ and $\mathbf{Q}_c(\mathbf{x}, \mathbf{x}') = 0$ are chosen, the estimation task for a spatial GP model could be solved by considering only one measurement step and using the same equations.

2. Hilbert Space Methods

The infinite-dimensional Kalman filtering and smoothing equations can be converted to a tractable form by either finite difference approximations or introducing Hilbert space methods (basis function approximations). The eigenfunction expansion of the linear operator is considered and combined with the infinite-dimensional framework. By truncating the expansion, a finite-dimensional approximate solution is obtained, which can be evaluated.

In the spatio-temporal resonator model, the negative Laplace operator can be considered in some spatial domain Ω subject to Dirichlet boundary conditions. This results in an eigenfunction equation in the form $-\nabla^2 \psi_n(\mathbf{x}) = \lambda_n \psi_n(\mathbf{x})$, where $\psi_n(\mathbf{x})$ is an eigenfunction and λ_n is the corresponding eigenvalue for each $n = 1, 2, \dots, N$ and spatial coordinate $\mathbf{x} \in \Omega$. The solution presented here $\mathbf{f}(\mathbf{x}, t)$ will be transformed to a new basis, which is given by the eigendecomposition of the linear operator in Ω . This new basis decodes the spatial structure so that only $\tilde{\mathbf{f}}(t)$ remains, being a finite-dimensional approximation of $\mathbf{f}(\mathbf{x}, t)$.

After the time-discretization step in (6), the finite-dimensional approximation of the s component model leads to a sN -dimensional state space model:

$$\begin{aligned}\tilde{\mathbf{f}}_{k+1} &= \mathbf{A}_k \tilde{\mathbf{f}}_k + \mathbf{q}_k \\ \mathbf{y}_k &= \mathbf{H}_k \tilde{\mathbf{f}}_k + \mathbf{r}_k,\end{aligned}$$

where the sparse dynamic model \mathbf{A}_k and the noise term $\mathbf{q}_k \sim \mathcal{N}(\mathbf{0}, \mathbf{Q}_k)$ are given in the basis defined by the eigenfunction expansion of \mathcal{F} in Ω (see the supplementary material in [15] for detailed equations). The explicit form of \mathbf{H}_k is determined by the basis functions evaluated at the observation locations \mathbf{x}^{obs} at time t_k .

E. Parameter Estimation

All the parameters needed in the model (typically the unknowns in the covariance function, the damping constants, and the measurement noise variance) are summarized as a vector quantity $\boldsymbol{\theta}$. For notational convenience, the parameters have not been explicitly written out in (8) and (9), but could be included as $\mathbf{U}(\Delta t, \boldsymbol{\theta})$, $\mathbf{Q}(\mathbf{x}, \mathbf{x}'; t, t'; \boldsymbol{\theta})$ and $\mathbf{R}_k(\boldsymbol{\theta})$. Based on these results, the marginal likelihood of the measurements can be computed, given $\boldsymbol{\theta}$ (see, *e.g.*, [23]):

$$p(\mathbf{y}_1, \dots, \mathbf{y}_T | \boldsymbol{\theta}) = \prod_{k=1}^T \mathcal{N}(\mathbf{y}_k | \mathcal{H}_k \mathbf{m}_{k|k-1}(\mathbf{x}, \boldsymbol{\theta}), \mathbf{S}_k(\boldsymbol{\theta})).$$

Hence, the marginal log-likelihood function for maximum likelihood (ML) estimation can be given with the help of the predicted mean $\mathbf{m}_{k|k-1}(\mathbf{x}, \boldsymbol{\theta})$ and the innovation

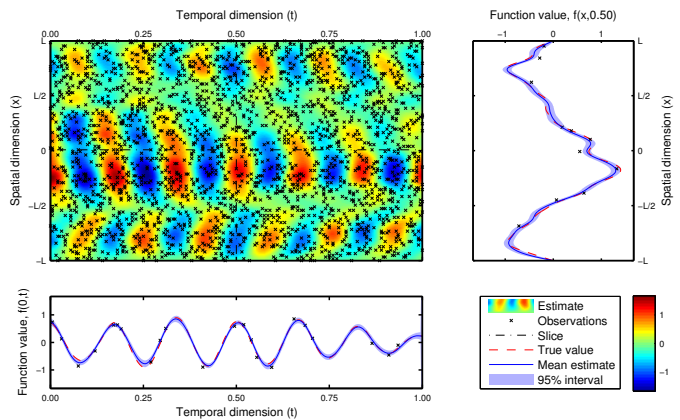


FIG. 1. This figure illustrates an example of a stochastic resonator realization in one spatial dimension. The left-hand figure shows the observation locations and the corresponding estimate of the oscillating field. The state at $t = 0.50$ s is shown in the right-hand figure, where the estimate is presented together with the dashed true values of the process.

covariance $\mathbf{S}_k(\boldsymbol{\theta})$ in (8) and (9):

$$\begin{aligned}\ell(\boldsymbol{\theta}) &= -\frac{1}{2} \sum_{k=1}^T \log |2\pi \mathbf{S}_k(\boldsymbol{\theta})| - \frac{1}{2} \sum_{k=1}^T (\mathbf{y}_k - \mathcal{H}_k \mathbf{m}_{k|k-1}(\mathbf{x}, \boldsymbol{\theta}))^\top \\ &\quad \times \mathbf{S}_k^{-1}(\boldsymbol{\theta}) (\mathbf{y}_k - \mathcal{H}_k \mathbf{m}_{k|k-1}(\mathbf{x}, \boldsymbol{\theta})).\end{aligned}\quad (11)$$

The parameter estimation problem now reverts to the maximization of the log-likelihood function: $\hat{\boldsymbol{\theta}} = \arg \max_{\boldsymbol{\theta}} \ell(\boldsymbol{\theta})$.

Using the log-likelihood function, the un-normalized posterior distribution could also be formed easily, which would allow the computation of maximum a posteriori (MAP) estimates or the use of a Metropolis–Hastings type of Markov chain Monte Carlo (MCMC) for integration over the parameters.

III. RESULTS

A. Illustrative One-Dimensional Example

Visualizations for simulated data in one spatial dimension are shown in Fig. 1 as an example of the spatio-temporal resonator model. The model contains one resonator $f(x, t)$ oscillating at a frequency of 6 Hz, where $x \in [-L, L]$ over a time-span $t \in [0, 1]$ (in seconds).

The Matérn covariance function is considered (see, *e.g.*, [12]) for the perturbing dynamic noise. This class of stationary isotropic covariance functions is widely used in many applications and their parameters have understandable interpretations. A Matérn covariance function can be expressed as:

$$C(r) = s^2 \frac{2^{1-\nu}}{\Gamma(\nu)} \left(\sqrt{2\nu} \frac{r}{l} \right)^\nu K_\nu \left(\sqrt{2\nu} \frac{r}{l} \right), \quad (12)$$

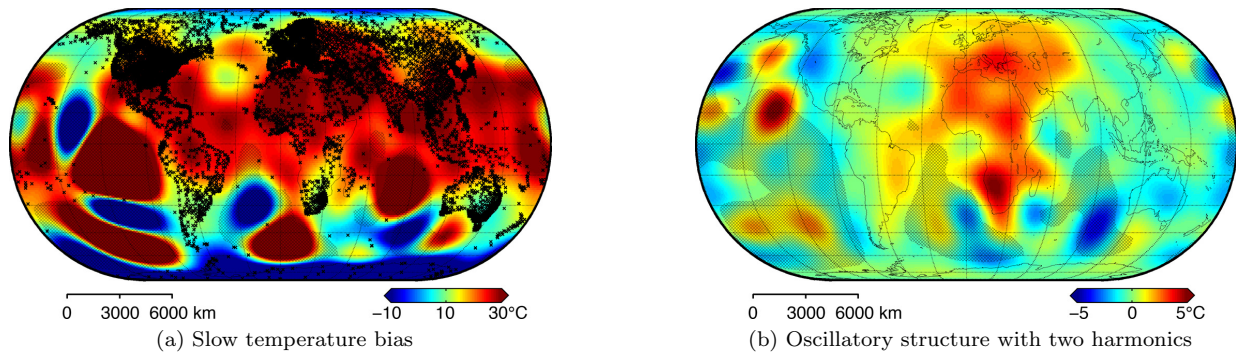


FIG. 2. Slow bias and resonator maps for temperatures as a snapshot on July 8, 2011 at 2 PM (GMT). The weather stations are marked with crosses and areas of uncertainty are hatched.

where $r = \|\mathbf{x} - \mathbf{x}'\|$, $\Gamma(\cdot)$ is the Gamma function and $K_\nu(\cdot)$ is the modified Bessel function. The covariance function is characterized by three parameters: a smoothness parameter ν , a distance scale parameter l , and a strength (magnitude) parameter σ , all of which are positive.

For simulating data, the model parameters were chosen so that $\gamma = 1$ and $\chi = 0.01$. The perturbing dynamic noise covariance function parameters were: $\nu = 3/2$, $l = 0.1L$, and $s = 25$. The Gaussian measurement noise variance was $\sigma^2 = 0.1^2$. A truncated eigenfunction decomposition with 32 eigenfunctions was used. Altogether, 2500 noisy observations were considered.

The model parameters are fitted by optimizing the marginal log-likelihood (11) using a conjugate gradient optimizer and square root versions of the filtering equations (8)–(10) for numerical stability. To avoid bad local minima, ten random restarts were attempted, and the run with the best marginal likelihood was selected. The optimized parameters were $\hat{\sigma}^2 \approx 0.098^2$, $\hat{l} \approx 0.106L$, $\hat{s} \approx 30.8$, $\hat{\gamma} \approx 0.690$, and $\hat{\chi} \approx 0.015$.

Fig. 1 shows the estimation mean $m(x, t)$ of the true space–time oscillating field $f(x, t)$ as a color surface plot. The measurement locations in space–time are shown as crosses. The oscillatory behavior is clear, and even clearer along the slice $x = 0$, which is shown in the lower figure. A slice $f(x, 0.5)$ along the spatial dimension is shown on the right. Both slices contain the true values for f (dashed), the estimate mean (solid), and a shaded 95% uncertainty interval.

B. Weather Data on the Surface of the Globe

In this section, the proposed methods are applied to hourly observations of temperature readings in centigrade, which were collected worldwide by *National Environmental Satellite, Data, and Information Services* (NESDIS)[24]. A subset of the data was considered consisting of hourly temperature measurements for one month (July, 2011), resulting in a time series of 745 tem-

poral points. The temperatures were recorded at 11 344 different spatial locations, for which the longitudinal and latitudinal coordinates are known and assumed exact. The locations of the stations are marked as crosses in Fig. 2a. However, not all stations provide hourly data; altogether there are 5 637 501 measurements.

A model with three latent components $f_j(\mathbf{x}, t)$ was used. The first latent component, a bias term with exponentially decaying memory, accounts for the slow drifting of the mean temperature, and the other two are oscillatory components for the daily variation of temperature. The first of these two oscillates at the constant base frequency of 1/day, and the second is the first harmonic (frequency 2/day). Similarly as in [4], the bias term was constructed as an oscillator with zero frequency. This corresponds to a spatio-temporal Wiener velocity model. The spatial covariance function of the process noise was fixed to the squared-exponential covariance function.

The model parameters (covariance function magnitudes, length scales, and the Gaussian measurement noise variance) were all optimized with respect to marginal likelihood using a few random restarts to avoid bad local minima. The damping parameters were virtually zero in all runs, therefore they were fixed to zero in the final model. This means that the spatial dependencies stem from the perturbation structure alone.

The estimation results for the temperature oscillation model are presented here as a snapshot of the temperature map over the globe on July 8, 2011 at 2 PM (GMT). The results in Fig. 2 are split into two in order to show the influence of the slow-moving bias and the resonating part. Fig. 2a also shows the spatial locations of the weather stations. The hatched regions indicate uncertainty (standard deviation $> 2^\circ\text{C}$), which corresponds to the regions with very few or no observations.

This test setup is subject to many simplifications and assumptions, which affect the results; the surface of the Earth is actually not a symmetrical sphere and the evident fact that the fluctuation covariance structure is not stationary is disregarded. However, the setup clearly captures two effects: the summer on the northern hemi-

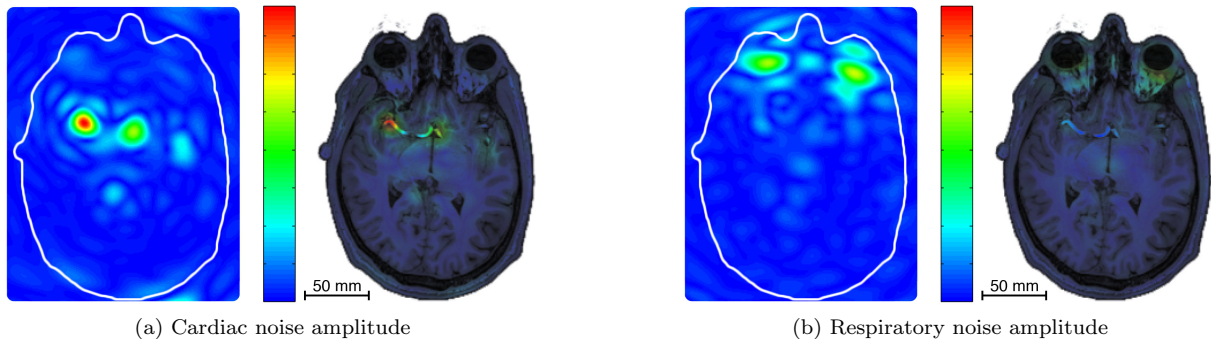


FIG. 3. Mean amplitude maps for the physiological noise components. The results are shown both in isolation and overlaid on top of the corresponding anatomical image.

sphere and the day–night variation (afternoon in Europe and Africa in the figure).

C. Modeling Pulsations in the Brain

Recent advances in *functional magnetic resonance imaging* (fMRI) techniques have demonstrated the importance of computational methods in modeling brain data. In [4], it was shown that eliminating oscillating physiological noise components in fMRI can be achieved by using a spatially independent resonator model combined with Kalman filtering. This method was named DRIFTER. This approach is now extended by showing how to account also for spatial dependencies.

One ~ 30 s run of empirical fMRI data was considered. The set of fast-sampled data of one slice is used here to demonstrate the spatio-temporal resonator model in two-dimensional polar coordinates. This fMRI data, together with anatomical images for one volunteer, were obtained using a 3 T scanner (Siemens Skyra) located at the *Advanced Magnetic Imaging Centre* (AMI) of Aalto University School of Science using a 32-channel receive-only head coil. For the functional imaging, the major parameters were repetition time (TR) 77 ms, echo time (TE) 20 ms, flip angle (FA) 60° , field-of-view (FOV) 224 mm, and matrix size 64×64 . The measurements were performed as part of AMI Centre’s local technical methods development research and conformed to the guidelines of the Declaration of Helsinki. The research was approved by the ethical committee in the Hospital District of Helsinki and Uusimaa.

In order to simulate resting state conditions, the stimulus was a fixed dot in the center of the visual field of the volunteer. The heart and respiratory signals were recorded, and time-locked to the fMRI data during the run. The oscillation frequency of the physiological noise components was quasi-periodic (rather than exactly periodic), which implies that the frequencies change over time. External reference signals with the *interacting multiple model* (IMM) approach, presented in [4], were used to estimate the frequency time series of heart beats and

respiration cycles. The cardiac frequency alternated between 54–64 beats per minute and the respiratory frequency between 6–15 cycles per minute.

One slice of fast-sampled fMRI data was used. The sampling interval was 0.077 s and the whole 64×64 matrix was observed during each of 350 time steps. The spatial domain Ω was chosen to be a circular disk with a radius of ≈ 155 mm. The spatio-temporal resonator model has three components: a slowly moving brain blood-oxygen-level-dependent (BOLD) signal—which also includes scanner drift and other slow phenomena—modeled with a spatio-temporal Wiener velocity model (see Sec. III B), and two space–time resonators oscillating at the time-dependent cardiac and respiratory frequencies, respectively. Here, only the resonators for the base frequencies were included; more complex signals could be accounted for by including harmonics. An eigenfunction decomposition of the linear operators in Ω with 300 eigenfunctions was used for each of the three components. Model parameters were chosen by studying the spatially independent model first.

Figure 3 shows the spatial amplitude of physiological noise contribution averaged over time. The results resemble the maps in [5], where the oscillators were assumed to be spatially independent and only the final results were spatially smoothed. This suggests that the method is able to capture the space–time structure of the oscillations. The cardiac influence is strong near the large cerebral arteries (see Fig. 3a), and the respiration causes artifacts near the eyes that are partly induced by movement.

IV. CONCLUSION AND DISCUSSION

This paper proposed a computationally effective stochastic partial differential equation model and an inference method for detecting and modeling latent oscillatory structures in spatio-temporal data. It showed how a physical first-principles SPDE model for spatio-temporal oscillations can be constructed, and how the Bayesian inference can be effectively applied using

infinite-dimensional Kalman filtering and Hilbert space methods. This filtering is related to Gaussian process regression and Hilbert space valued stochastic processes. The proposed method allows a reduction of the complexity of a direct GP solution from cubic to linear with respect to measurements in the temporal dimension.

A truncated eigenfunction expansion of the Laplace operator was used to form a finite-dimensional basis over the spatial domain, which made it possible to revert to the traditional Kalman filtering scheme. The eigenfunction expansions of the Laplace operator in both spherical and Cartesian coordinates were used in the numerical computations.

The numerical results show that the truncated expansion puts some restrictions on the spatial short-scale variability. The basis function approach tends to make the model spatially smooth, a problem that has been dealt with before in many ways under the GP regression scheme (see, *e.g.*, [12]). However, in many applications such as in functional brain data analysis, this is not a problem since a few hundred basis functions are sufficient to match the required spatial resolution.

Several methodological extensions could be considered: In temporal sense, a broad family of quasi-periodic oscillations can be modeled by including a sufficient number of harmonics. Non-linear oscillator models can also be approximated, if the realizations are periodic. This applies, for example, to relaxation oscillators such as systems generated by the Van der Pol oscillator. Other properties of the stochastic oscillator model [4] also apply to

this spatial extension of it. In Sec. III C the oscillation frequency was time-dependent, and it would be possible to extend the model to account for different regions of the spatially extended system oscillating at different frequencies. Including non-stationary covariance functions in the process noise term would provide many extensions to the perturbation model structure. Spatially, relaxing the coupling between operators \mathcal{A} and \mathcal{B} allows various spatio-temporal models to be accounted for. For example, if we consider in Eq. (4) $\gamma_j = \chi_j = 0$, but $\gamma_j \chi_j > 0$, the model corresponds to an undamped oscillating field, where the perturbations follow wave equation dynamics. The inference scheme is also compatible with this type of models, which can be useful, for example, in modeling of epidemic spread.

In general, the spatio-temporal model can mitigate the problems related to slow sampling rates, because the spatial information can compensate for missing temporal data. This turns such models into powerful tools for signal reconstruction and noise elimination, for example in fMRI studies, especially as the computational complexity grows only linearly with the length of the measurement session.

ACKNOWLEDGMENTS

The authors would like to thank Simo Vanni, Ari Laiho, and Toni Auranen for their help with data acquisition, and Aki Vehtari and Fa-Hsuan Lin for some helpful discussions of the topic. We also acknowledge the computational resources provided by the Aalto Science-IT project.

-
- [1] H. Rotermund, W. Engel, M. Kordesch, and G. Ertl, *Nature* **343**, 355 (1990).
 - [2] Y. A. Rzhannov, H. Richardson, A. A. Hagberg, and J. V. Moloney, *Physical Review A* **47**, 1480 (1993).
 - [3] R. Singh and S. Sinha, *Physical Review E* **87**, 012907 (2013).
 - [4] S. Särkkä, A. Solin, A. Nummenmaa, A. Vehtari, T. Auranen, S. Vanni, and F.-H. Lin, *NeuroImage* **60**, 1517 (2012).
 - [5] S. Särkkä, A. Solin, A. Nummenmaa, A. Vehtari, T. Auranen, S. Vanni, and F.-H. Lin, in *Proceedings of ISMRM 2012*, 1535 (The International Society for Magnetic Resonance in Medicine, 2012).
 - [6] K. Burrage, I. Lenane, and G. Lythe, *SIAM journal on scientific computing* **29**, 245 (2008).
 - [7] J. Hartikainen, M. Seppänen, and S. Särkkä, in *In Proceedings of the 29th International Conference on Machine Learning (ICML 2012)* (2012).
 - [8] J. K. Hale, *Journal of Dynamics and Differential Equations* **9**, 1 (1997).
 - [9] G. E. P. Box, G. M. Jenkins, and G. C. Reinsel, *Time Series Analysis: Forecast and Control*, 4th ed., Wiley series in probability and statistics (John Wiley & Sons, 2008).
 - [10] R. Pindyck and D. Rubinfeld, *Econometric Models and Economic Forecasts*, Vol. 2 (McGraw-Hill, New York, 1981).
 - [11] S. Haykin, *Neural Networks: A Comprehensive Foundation*, 2nd ed. (Upper Saddle River (NJ): Prentice Hall, 1999).
 - [12] C. E. Rasmussen and C. K. I. Williams, *Gaussian Processes for Machine Learning* (The MIT Press, 2006).
 - [13] J. Quiñero-Candela and C. E. Rasmussen, *Journal of Machine Learning Research* **6**, 1939 (2005).
 - [14] F. Lindgren, H. Rue, and J. Lindström, *JRSS B* **73**, 423 (2011).
 - [15] S. Särkkä and J. Hartikainen, in *JMLR Workshop and Conference Proceedings Volume 22: AISTATS 2012* (2012) pp. 993–1001.
 - [16] G. Da Prato and J. Zabczyk, *Stochastic Equations in Infinite Dimensions*, Encyclopedia of Mathematics and its Applications, Vol. 45 (Cambridge University Press, 1992).
 - [17] S. Särkkä, *Bayesian Filtering and Smoothing*, Institute of Mathematical Statistics Textbooks, Vol. 3 (Cambridge University Press, 2013).
 - [18] P. Chow, *Stochastic Partial Differential Equations*, Chapman & Hall/CRC applied mathematics and nonlinear science series, Vol. 11 (Chapman & Hall/CRC Press, 2007).
 - [19] S. G. Tzafestas, in *Distributed Parameter Systems: Identification, Estimation and Control*, edited by W. H. Ray

- and D. G. Lainiotis (Marcel Dekker, Inc., New York, 1978).
- [20] S. Omatu and J. H. Seinfeld, *Distributed Parameter Systems: Theory and Applications* (Clarendon Press / Ohmsha, 1989).
- [21] N. Cressie and C. K. Wikle, in *Encyclopedia of Environmental Metrics*, Vol. 4, edited by A. H. El-Shaarawi and W. W. Piegorsch (John Wiley & Sons, Ltd, Chichester, 2002) pp. 2045–2049.
- [22] M. S. Grewal and A. P. Andrews, *Kalman Filtering: Theory and Practice Using MATLAB*, 2nd ed. (Wiley-Interscience, 2001).
- [23] H. Singer, *ASTA Advances in Statistical Analysis* **95**, 375 (2011).
- [24] The dataset is available for download from U.S. National Climatic Data Center: <http://www7.ncdc.noaa.gov/CD0/cdoselect.cmd> (accessed December 12, 2011).